

Electrochemiluminescence Study of Perovskite -type oxides LaTiO₃-Ag_{0.1} with Ru(bpy)₃²⁺ modified electrode

Yin-zhu Wang^{1,2}, Hui Zhong^{1,2,3,*}, Xiao-mo Li^{2,3}, Fei-fei Jia^{2,3}, Bao-chen Ding^{1,2}, Bin Gu^{1,2}, Wei-guang Zhan², Zhi-peng Cheng², Li-li Zhang², Shu-ping Li⁴, Ji-kui Wang^{1*}

¹ College of Sciences, Nanjing University of Technology, Nanjing 210009, P. R. China

² Jiangsu Key Laboratory for Chemistry of Low-Dimensional Materials, School of Chemistry & Chemical Engineering, Huaiyin Normal University, Huaian 223300, P. R. China

³ Faculty of Chemistry, Northeast Normal University, Changchun 130024, People's Republic of China

⁴ Jiangsu Key Laboratory of Biofunctional Material, College of Chemistry and Material Science, Nanjing Normal University, Nanjing, 210097, China

*E-mail: huizhong@hytc.edu.cn, wjk@njut.edu.cn

Received: 30 September 2012 / Accepted: 31 December 2012 / Published: 1 February 2013

The unique perovskite-type oxides LaTiO₃-Ag_{0.1} was synthesized and used to combine with Tris(2,2'-bipyridyl)ruthenium(II) on a glassy carbon electrode as an electrochemiluminescence(ECL) sensor. Ru(bpy)₃²⁺ was firmly immobilized on the surface of the electrode due to the large specific surface of LaTiO₃-Ag_{0.1} and the electrostatic interaction. The immobilized Ru(bpy)₃²⁺ could maintain its ECL behavior in response to the co-reactants tripropylamine(TPA) and had high sensitivity. The ECL sensor showed a good linear range from 6.4 nM to 1.1 μM and the detection limit was 1 nM (S/N=3). The detection limit was about 2 orders of magnitude lower than that of previously reported methods TiO₂ or SiO₂ for the determination of TPA. The ECL sensor presented good characteristics in terms of sensitivity and stability. This work provided a new application of mixed metal oxides to ECL and bridged the inorganic mixed metal oxides and electrochemiluminescence.

Keywords: Nanocomposite; Sensors; Luminescence; perovskite-type oxides

1. INTRODUCTION

Electrochemiluminescence(ECL) of tris(2,2'-bipyridyl) ruthenium(II) has been one of the most highly studied ECL compounds due to its inherent high detection sensitivity, low background signal and simplified optical setup [1]. Ru(bpy)₃²⁺-based ECL has been used extensively to detect a wide range of compounds such as NADH [2], oxalate [3], amines [4] and other compounds containing

tertiary amine functional groups [5,6]. The critical importance of $\text{Ru}(\text{bpy})_3^{2+}$ study is to facilitate its application.

In recent years, solid-state $\text{Ru}(\text{bpy})_3^{2+}$ -ECL has been developed. Compared with solution phase $\text{Ru}(\text{bpy})_3^{2+}$ system, it has enhanced the ECL signal, saved the expensive reagent and simplified the setup [7,8]. Several materials and methods have been used to immobilize $\text{Ru}(\text{bpy})_3^{2+}$, such as ion-exchange polymer Nafion [9], sol-gel matrix [10], Langmuir–Blodgett(LB) [11], carbon nanotube [12] and so on. Thus, new materials and new approaches with more advantages are still crucial to the research.

Metal oxides have been widely used in the field of immobilized electrodes such as SiO_2 and TiO_2 and exhibited outstanding advantages concerning both sensitivity and stability[13, 14]. Relative to metal oxide, mixed metal oxides have been widely used in the field of heterogeneous catalysis. Different types of tailor-made mixed metal oxides with different solid state, surface and morphological properties are used in heterogeneous catalysis. Among such a wide range of mixed metal oxides, perovskite and perovskite-type oxides remain distinguished.

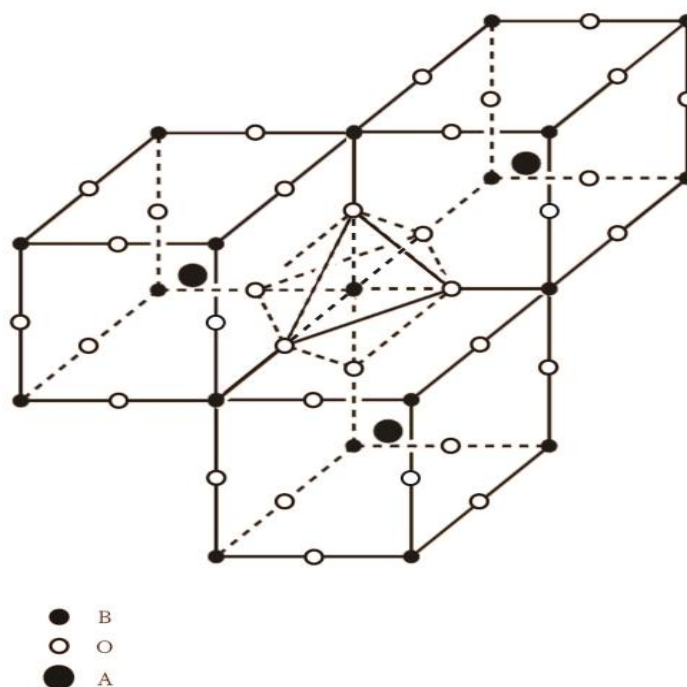


Figure 1. Ideal perovskite structure illustrated for ABO_3 . Note the corner-shared octahedra, extending in three dimensions.

Perovskite-type oxides ABO_3 (where A is usually a rare earth and B a transition metal) shown in Fig. 1 is that A –site cation fills the 12 coordinate cavities formed by BX_3 net work and is surrounded by 12 equidistant anions [15]. Perovskite-type oxides ABO_3 has been paid much attention to due to its special characteristics such as ion exchange properties, absorption properties, catalytic potential, high surface-volume ratio and porosity, good thermal stability and redox properties [16].

Fuel cell cathode materials, pollution abatement, chemical sensor, and electrocatalysis are all the areas that perovskite-type oxides ABO_3 has been applied to [17].

Rare-earth perovskites containing transition ions show wide differing electrical properties, and $LaTiO_3$ exhibits collective d-electron behavior and shows a metallic conductivity and Pauli paramagnetism [13]. Ag(I) was mixed into $LaTiO_{3+\lambda}$ to replace a part of La^{3+} so that the electronic transmission performance can be improved. The cation defect of perovskite-type oxide $LaTiO_{3+\lambda}$ was used for synthesis of perovskite-type oxide $LaTiO_3-Ag_{0.1}$. A-site of $LaTiO_{3+\lambda}$ could be replaced by other types of atoms in order to adjust the density of vacancies.

In this work, tailor-made perovskite-type oxide $LaTiO_3-Ag_{0.1}$ is presented. Rare-earth perovskite $LaTiO_3$ shows a metallic conductivity and the addition of Ag(I) enhances the ECL. We use nano-level negatively charged $LaTiO_3-Ag_{0.1}$ to immobilize $Ru(bpy)_3^{2+}$ on the surface of glassy carbon electrode (GCE) through electrostatic interaction. The modified electrode is used to determine TPA with the advantage of sensitive and stable.

2. EXPERIMENTAL

2.1. Reagents

Tripropylamine (TPA) and tris(2,2'-bipyridyl)dichlororuthenium hexahydrate ($Ru(bpy)_3Cl \cdot 6H_2O$) were purchased from Aldrich. The buffer solution was a 0.2 M phosphate buffer solution (pH 8.0). All reagents were of analytical grade and were used without purification. In the typical synthetic process, 0.39 g of $La(NO_3)_3 \cdot 6H_2O$ and 0.017 g of $AgNO_3$ were dissolved in 40 mL of absolute ethanol. The solution was stirred with a magnetic stirrer for 10 min to ensure that the $La(NO_3)_3$ and $AgNO_3$ completely dissolved. Under constant stirring, 5.7 mL of butyl titanate was dropped into the $La(NO_3)_3$ and $AgNO_3$ solution at room temperature. Subsequently, the above solution was transformed into a Teflon-lined stainless steel autoclave (50 mL capacity) maintained at 180 °C for 24 h, and cooled to room temperature naturally. After filtration and washing, the residue was dried and calcined in a muffle furnace at 800 °C for 6 h. Distilled water was purified with a Millipore system (Millipore Co. USA) and used in all aqueous solution preparations and washing.

2.2. Instrumentation

The surface charge of $LaTiO_3-Ag_{0.1}$ was characterized by the zeta potential (Brookhaven Instrument Company). Electrochemical measurements were performed in a three-electrode cell (volume 0.5 ml) with an Autolab PGSTAT30 analyzer (EcoChemie, Utrecht, The Netherlands). The working electrode was $Ru(bpy)_3^{2+}$ modified GCE with a Pt wire electrode as the auxiliary and a $Ag|AgCl(sat.KCl)$ as the reference. The corresponding ECL was detected by a Model MPI-A CE-ECL Analyzer System (Xi'an Remax Electronic High-Tech Ltd, Xi'an, China). The photomultiplier tube (PMT) was biased at 800 V. Unless noted otherwise, the PMT was biased at 800 V.

2.3. Preparation of the modified electrode

The $\text{LaTiO}_3\text{-Ag}0.1/\text{Ru}(\text{bpy})_3^{2+}$ modified electrode was prepared via the following procedures: first Glassy carbon electrode (GCE) was polished with 1, 0.3 and 0.05 μm α -alumina to a mirror finish. Then an 8 mg mL^{-1} $\text{LaTiO}_3\text{-Ag}0.1$ (5 μL) was dropped on the GCE surface and dried under ambient conditions for at least 24 h. And finally 5 mmol L^{-1} $\text{Ru}(\text{bpy})_3^{2+}$ (5 μL) was dropped on the perovskite film. After stored in dry state for 24 h, the GCE was modified. $\text{LaTiO}_3\text{-Ag}0.1/\text{Ru}(\text{bpy})_3^{2+}$ was modified on the GCE surface via good absorption properties and cation exchange properties.

3. RESULTS AND DISCUSSION

3.1. Characterization of $\text{LaTiO}_3\text{-Ag} 0.1$

SEM was used to characterize $\text{LaTiO}_3\text{-Ag}0.1$ nanoparticles. $\text{Ag}(\text{I})$ was mixed into $\text{LaTiO}_{3+\lambda}$ replaced a part of La^{3+} in order to improved the electronic transmission performance of $\text{LaTiO}_3\text{-Ag}0.1$. As shown in Fig. 1a, the nanoparticles were in uniform with the size and the $\text{LaTiO}_3\text{-Ag}0.1$ we synthesized was spherical particles. A part of La^{3+} was replaced by $\text{Ag}(\text{I})$ and the doped $\text{Ag}(\text{I})$ was saturated so that the $\text{LaTiO}_3\text{-Ag}0.1$ was in uniform too. Fig. 1b shows XRD characterization of $\text{LaTiO}_3\text{-Ag}0.1$. The peaks are pure and diffraction peaks move to lower angle position, which is probably due to the unit cell expansion by addition of $\text{Ag}(\text{I})$. The addition of $\text{Ag}(\text{I})$ substitutes the $\text{La}(\text{III})$ of A-site and maintains the charge balance. Its combination with the image of SEM illustrates that the reaction products are pure and consistent with the image of XRD. The negative charge surface of $\text{LaTiO}_3\text{-Ag}0.1$ is characterized by the zeta potential, and $\text{LaTiO}_3\text{-Ag}0.1$ has larger specific surface. The excessive silver and silver oxide are adhered to the surface of the crystal before the doped $\text{Ag}(\text{I})$ substitutes the $\text{La}(\text{III})$ of A-site to maintain the charge balance. Thus $\text{LaTiO}_3\text{-Ag}0.1$ can be used to immobilize positively charged $\text{Ru}(\text{bpy})_3^{2+}$ through interaction properties.

3.2. Electrochemical behavior of the immobilized $\text{Ru}(\text{bpy})_3^{2+}$

The sol-gel prepared $\text{LaTiO}_3\text{-Ag}0.1$ was directly coated with GCE surface and $\text{Ru}(\text{bpy})_3^{2+}$ was trapped in the $\text{LaTiO}_3\text{-Ag}0.1$ film. The $\text{LaTiO}_3\text{-Ag}0.1$ film can incorporate cations into solutions effectively and demonstrate several advantages, such as large specific surface, interaction properties, low cost, enhancement of ECL and catalytic potential. Composite film is used to modified GCE, which is based on the electrostatic interaction between positively charged $\text{Ru}(\text{bpy})_3^{2+}$ and negatively charged $\text{LaTiO}_3\text{-Ag}0.1$. Nano-level $\text{LaTiO}_3\text{-Ag}0.1$ can fix $\text{Ru}(\text{bpy})_3^{2+}$ firmly due to the large specific surface and electrostatic interaction. Owing to the electrocatalytic properties $\text{Ru}(\text{bpy})_3^{2+}$ diffuse rapidly in the membrane and accelerate the reaction. The electrochemical behavior of $\text{Ru}(\text{bpy})_3^{2+}$ immobilized in $\text{LaTiO}_3\text{-Ag}0.1$ matrix was studied by using cyclic voltammetry performed in solution with the modified electrode. $\text{LaTiO}_3\text{-Ag}0.1$ was cation exchangeable and had large specific surface while $\text{Ru}(\text{bpy})_3^{2+}$ is positively charged, thus this composite film of $\text{LaTiO}_3\text{-Ag}0.1$ and $\text{Ru}(\text{bpy})_3^{2+}$ can be

assembled by alternate adsorption when using $\text{LaTiO}_3\text{-Ag}0.1$ dispersions in water and $\text{Ru}(\text{bpy})_3^{2+}$ solution. The electrochemical ECL properties and analytical performance of the $\text{LaTiO}_3\text{-Ag}0.1/\text{Ru}(\text{bpy})_3^{2+}$ immobilized electrode were studied with oxalate as the coreagent, and the ECL can be enhanced by silver and silver(I) ions [14,18].

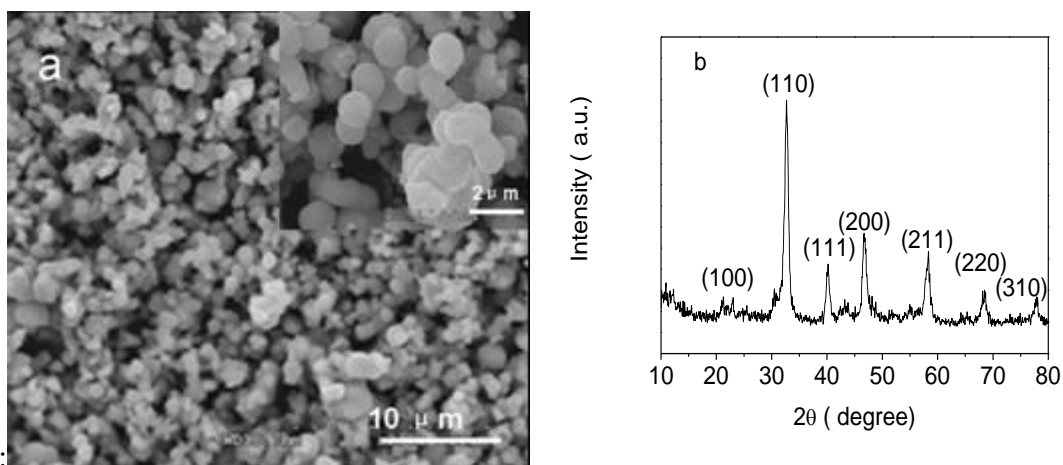


Figure 2. The SEM images of $\text{LaTiO}_3\text{-Ag}0.1$ (a) and XRD characterization of $\text{LaTiO}_3\text{-Ag}0.1$ (b).

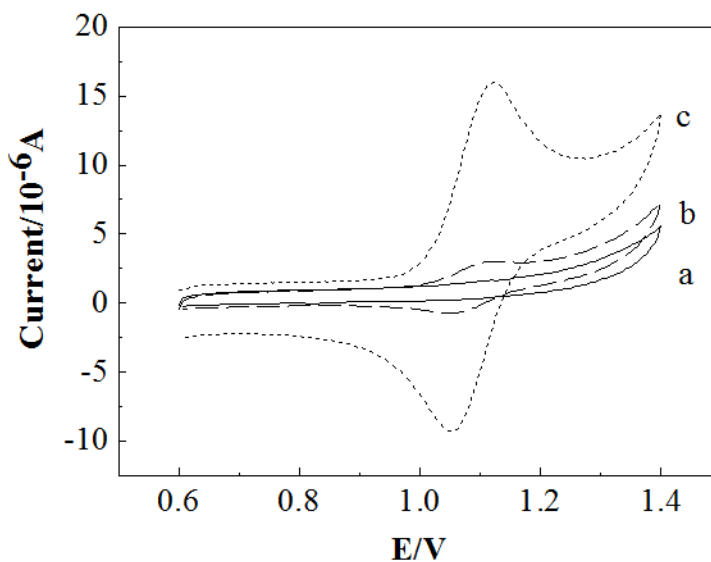


Figure 3. Cyclic voltammograms of the $\text{LaTiO}_3\text{-Ag}0.1$ modified electrode (a) in 0.2 M PBS (pH 6.8) and $\text{Ru}(\text{bpy})_3^{2+}$ doped $\text{LaTiO}_3\text{-Ag}0.1$ modified electrode in the absence (b) and presence (c) of 100 nM TPA at the scan rate of 50 mV/s.

Fig. 2 shows the cyclic voltammograms of the $\text{LaTiO}_3\text{-Ag}0.1$ immobilized electrode in 0.2 M PBS (pH 6.8) before (b) and after (c) dropped $\text{Ru}(\text{bpy})_3^{2+}$. There is no redox wave for $\text{LaTiO}_3\text{-Ag}0.1$ immobilized electrode before dropped with $\text{Ru}(\text{bpy})_3^{2+}$ (curve a). After dropped with $\text{Ru}(\text{bpy})_3^{2+}$ a pair of redox waves appeared and the anodic peak and cathodic peak increased dramatically (curve b). The

potential difference between reduction and oxidation is nearly 50 mV, which shows that $\text{Ru}(\text{bpy})_3^{2+}$ has still a good electrochemical reversibility after immobilized in $\text{LaTiO}_3\text{-Ag}0.1$ matrix. The anodic peak increased while the cathodic decreased in the presence of 100 nM TPA (curve c). The electrochemical equation is: $\text{Ru}(\text{bpy})_3^{2+} \rightarrow \text{Ru}(\text{bpy})_3^{3+} + \text{e}^-$. These results show that $\text{LaTiO}_3\text{-Ag}0.1$ matrix is an effective medium for the electrical transfer of $\text{Ru}(\text{bpy})_3^{2+}$ and the immobilized $\text{Ru}(\text{bpy})_3^{2+}$ shows excellent electrochemical properties, which is attribute to the metallic conductivity and the addition of Ag(I) [13,14]. This result further indicated that amounts of $\text{Ru}(\text{bpy})_3^{2+}$ had been incorporated into $\text{LaTiO}_3\text{-Ag}0.1$ matrix after being dropped by $\text{Ru}(\text{bpy})_3^{2+}$. $\text{LaTiO}_3\text{-Ag}0.1$ with large specific surface, good absorption properties and cation exchange properties can incorporate $\text{Ru}(\text{bpy})_3^{2+}$ well.

Fig. 3 shows the CV of the $\text{Ru}(\text{bpy})_3^{2+}/\text{LaTiO}_3\text{-Ag}0.1$ composite matrix in 0.2 M PBS(pH 6.8) at different scan rates. The anodic and cathodic peak currents are proportional to the scan rate over 0.05-0.5 mV/s, the linear equation is $y=9.978\text{E}^{-7} + 1.140\text{E}^{-5}$ (in set), indicating that the immobilized $\text{Ru}(\text{bpy})_3^{2+}$ was a surface-controlled process.

3.3 ECL applications towards TPA detection

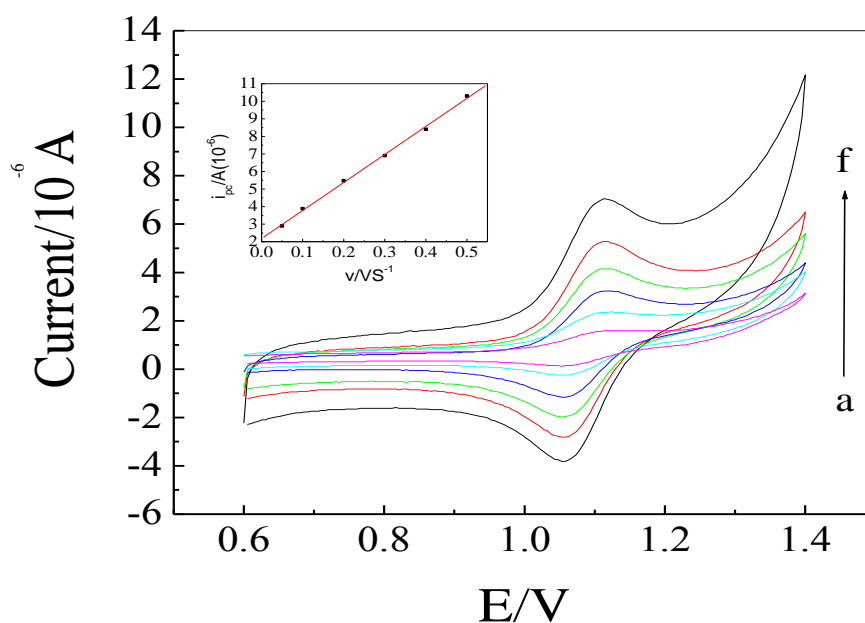


Figure 4. Fig. 4 Cyclic voltammograms of the electrode immobilized $\text{LaTiO}_3\text{-Ag}0.1/\text{Ru}(\text{bpy})_3^{2+}$ at various scan rates (from a to f curve: 0.05, 0.10, 0.20, 0.30, 0.40, 0.50 V s^{-1}) in 0.2 M PBS (pH=6.8). The inset is the relationship between the anodic peak currents and the square root of the scan rates.

The ECL process of $\text{LaTiO}_3\text{-Ag}0.1/\text{Ru}(\text{bpy})_3^{2+}$ modified electrodes with composite films in the presence of TPA showed great dependence on solution pH. Fig. 4 shows the influence of pH on the relative ECL intensity. The ECL was investigated from pH of 5.5 to 8.5 with the emission peak at pH

6.8. In addition, noise increases greatly at higher pH. Therefore, the pH of carrier solution was kept at pH 6.8. The strong pH dependence of the ECL suggested that the oxalate proton be necessary for LaTiO₃-Ag0.1/Ru(bpy)₃²⁺ ECL system of complex films, which was consistent with the mechanism proposed in the literature for producing solution-based ECL.

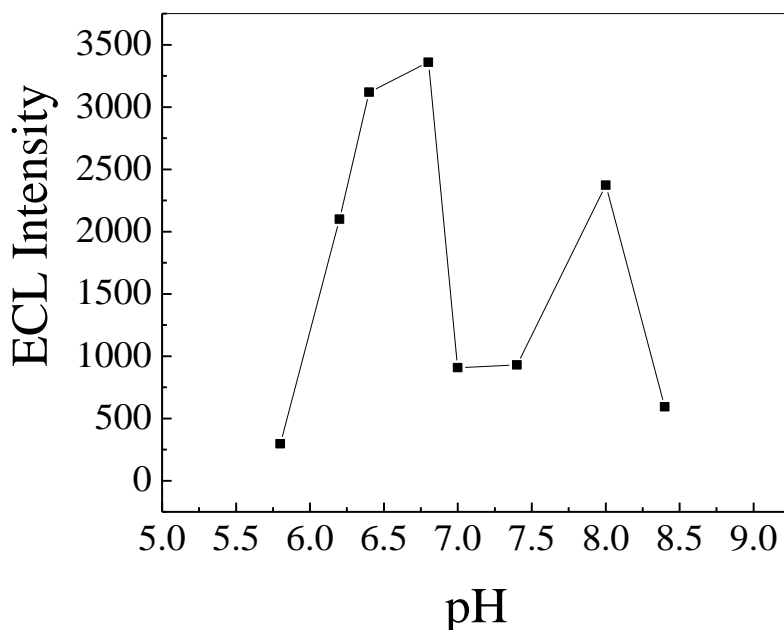


Figure 5. The effect of pH on ECL intensity in phosphate buffer solution containing 12mM oxalate. Scan rate 100 mVs⁻¹

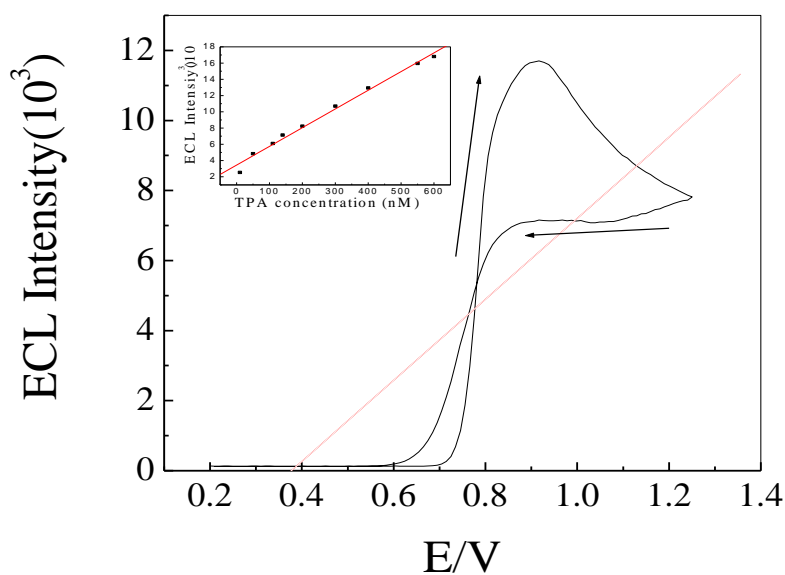


Figure 6. Corresponding ECL intensity-potential curve of the electrode immobilized LaTiO₃-Ag0.1/Ru(bpy)₃²⁺. The inset is the calibration curve of TPA.

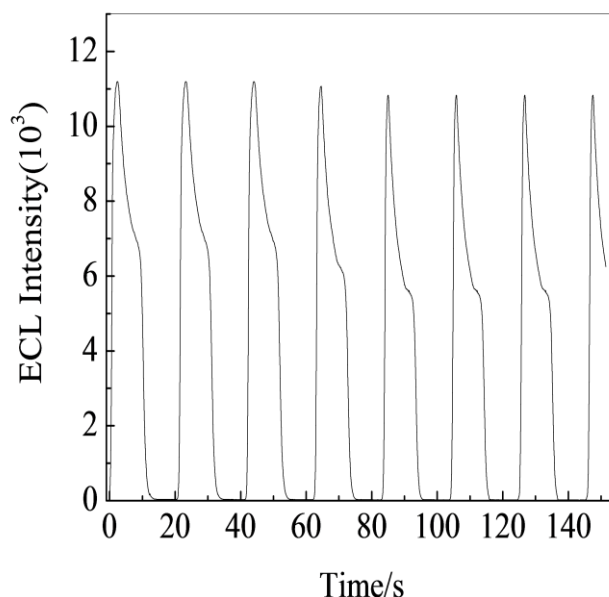


Figure 7. ECL emission from an $\text{LaTiO}_3\text{-Ag}0.1/\text{Ru}(\text{bpy})_3^{2+}$ modified GCE in PBS (pH 6.8) containing $10\ \mu\text{M}$ TPA. Scan rate of $100\ \text{mVs}^{-1}$.

Under optimum experimental, $\text{Ru}(\text{bpy})_3^{2+}$ -TPA system was used to examine the ECL properties of the immobilized electrode. As shown in Fig. 5, the onset of luminescence signal starts at 0.7 V and reaches the maximum at 0.9 V, which is consistent with the redox of the immobilized $\text{Ru}(\text{bpy})_3^{2+}$. The maximum ECL peak is about 12000 a.u. in the presence of $10\ \mu\text{M}$ TPA, which indicates that $\text{Ru}(\text{bpy})_3^{2+}/\text{LaTiO}_3\text{-Ag}0.1$ modified electrode exhibited excellent ECL behavior. As shown in set of Fig. 5, the linear range is from 6.4 nM to $1.1\ \mu\text{M}$ with a detection of 1 nM(S/N=3). Compared with TiO_2 and SiO_2 modified electrode, the penetration of $\text{Ru}(\text{bpy})_3^{2+}$ into the $\text{LaTiO}_3\text{-Ag}0.1$ has a synergistic effect [19, 20]. As shown in Fig. 6, no obvious decrease was observed in the ECL intensity. The result suggested that $\text{LaTiO}_3\text{-Ag}0.1/\text{Ru}(\text{bpy})_3^{2+}$ immobilized GCE be quite stable due to the electrostatic interaction between $\text{LaTiO}_3\text{-Ag}0.1$ and $\text{Ru}(\text{bpy})_3^{2+}$. Electrostatic interactions between negatively charged $\text{LaTiO}_3\text{-Ag}0.1$ and positively charged $\text{Ru}(\text{bpy})_3^{2+}$ may also decrease the ligand π - π energy gap and raise the quantum efficiency of reaction [14].

4. CONCLUSIONS

In summary, the new perovskite-type oxide $\text{LaTiO}_3\text{-Ag}0.1$ is used for ECL sensor and the cross-fertilization can become a new direction of perovskite-type oxides. The $\text{Ru}(\text{bpy})_3^{2+}/\text{LaTiO}_3\text{-Ag}0.1$ modified electrode is stable with wide linear range and low detection limit. Perovskite-type oxides can also be used to immobilize some positively charged biomolecules to develop biosensors and bioreactors. The study shows that perovskite-type oxides has a great promise for ECL applications.

ACKNOWLEDGEMENTS

This work was supported by National Natural Science Foundation of China (20975043, 21073093, 51106061) and Jiangsu Province (BK2010289), Jiangsu Higher Institutions Key Basic Research Projects of Natural Science(09KJA530001, 10KJA430005) and the “Qinglan” Project of Jiangsu Province (2010).

References

1. M. M. Richter, *Chem. Rev.* 104 (2004) 3003.
2. A. Chovin, P. Garrigue, N. Sojic, *Bioelectrochemistry*, 69 (2006) 25.
3. I. Rubinstein, A.J.Bard, *Anal.Chem.*55 (1983) 1580.
4. K. Uchikura, M. Kirisawa, *Anal. Sci.* 7 (1991) 803.
5. G. M. Greenway, A.W. Knight, P.J. Knight, *Analyst.* 120 (1995) 2549.
6. J. M. Gonzalez, G. M. Greenway, T. McCreedy, Q. J. Song, *Analyst.* 125 (2000) 765.
7. L. Lshultz, J.S. Stoyanoff and T.A.Nieman, *Anal Chem.* 68 (1996) 349.
8. B. Gu, H. Zhong, L. L. Zhang, *Int. J. Electrochem. Sci.* 7 (2012) 6202.
9. T. M. Downey, T. A. Nieman, *Anal. Chem.* 64 (1992) 261.
10. A. N. Khramov, M. M. Collinson, *Anal. Chem.* 72 (2000) 2943.
11. C. J. Miller, P. McCord, A. J. Bard, *Langmuir.* 7 (1991) 2781.
12. C.A. Li, K. N. Han, M. P. N. Bui, X.H. Pham, G. H. Seong, *Appl.Surf. Sci.* 256 (2010) 7428.
13. M. A. Pena, J. L. G. Fierro, *Chem Rev.* 101 (2001) 1981.
14. B. A. goman, P. S. rancis, D.E. Dunstan, N. W. Barnett, *Chem. Commun.* 4 (2007) 393.
15. O. Muller, R. Roy, The major ternary Structural Families, *SpringerVerlag*, (1974) 55.
16. S. Chopraa, S. Sharmaa, T.C. Goel, R.G. Mendiratta, *Materials Chemistry and Physics* 91 (2005) 161.
17. R. Singh, T.C. Goel, S. Chandra, *Materials Chemistry and Physics*, 110 (2008) 120.
18. L. Qian, X. yang, *Talanta.*73 (2007) 189.
19. L. Zhang, S. Dong. *Chem. Commun* 78 (2006) 5119.
20. Y. Zhuang, H. Ju, *Electroanalysis*, 16 (2004) 1401.